	Expanded	Compressed	Ratio
Magnification	1.4	0.65	2.2
Receptive Field Size	30	44	0.68
Mean Response Strength	15	8.5	1.8
Proportion Above Mean	0.47	0.48	0.98

Table 3.1: Map magnification and receptive field properties for expanded and compressed maps.

field strength for each source location was determined by stimulating a cluster of 5 source neurons centered at that location,[8] and allowing activation to spread laterally in the target. Four properties of the final maps were measured:

1. The average spacing between nodes was used as a measure of map magnification.
2. The average number of source locations to which a target node responds was used as a measure of its receptive field size.
3. The mean response strength to locations within the receptive field was measured separately for each target node, and these values were averaged to determine the average mean response strength.
4. The proportion of source locations for which the response strength was greater than the mean response strength for that target was used as a rough measure of receptive field shape.

Results are shown in Table 3.1. This data indicates that the general shape of the receptive fields is unchanged by usage-dependent map expansion and compression; however, their size and average strength are strongly affected. The strength of the receptive fields increases as the map expands, and the receptive field size decreases. These properties are similar to biological results in that map magnification and re-

[8] This is the same size that was used to drive map formation.

ceptive field size change in opposite directions. However, the proportional difference in receptive field size is considerably smaller than the magnification difference.

This may, in part, reflect a difference between properties of normal cortical maps and properties of experimentally manipulated maps. Magnification of normal cortical maps varies in proportion to the receptor density in the corresponding source region [31]. In the experimental situation, the usage of a source region is modified, but there is no corresponding change in receptor density. This could affect the relative change in receptive field size as the map expands or compresses.

Lesion Studies

Another change is necessary to run lesion studies. Up to this point, the formation of new synapses has not been included in this model. Because of this, it is necessary to ensure that the location of the initial arbor overlaps the desired final location. However, if some part of the source or target structure is lesioned, the desired final location of some arbors is quite far from their initial location, so it is necessary to include some form of synapse formation. An extremely simple mechanism for synapse formation is used, on the assumption that if it is sufficient, any more realistic model is also likely to work. The scheme used is to add new connections, with initially random weights, from active source neurons to the immediate neighbors of active target neurons. This pattern of synapse formation might result if the source axon were to "sprout" new terminals in the vicinity of a synapse that is being strengthened; these terminals could then make connections with nearby dendrites of neighboring cells.[9]

This scheme, though extremely simplistic, is sufficient to allow map expansion and migration into unused tissue after a source lesion, and map compression after a target lesion (see Figures 3-8 and 3-9).

[9] The model described in [50], for example, uses a similar form of synaptic sprouting as an integral part of its learning mechanism. In the optic tectum in the frog, new synapse formation has been hypothesized as a primary mechanism for the map development [11].

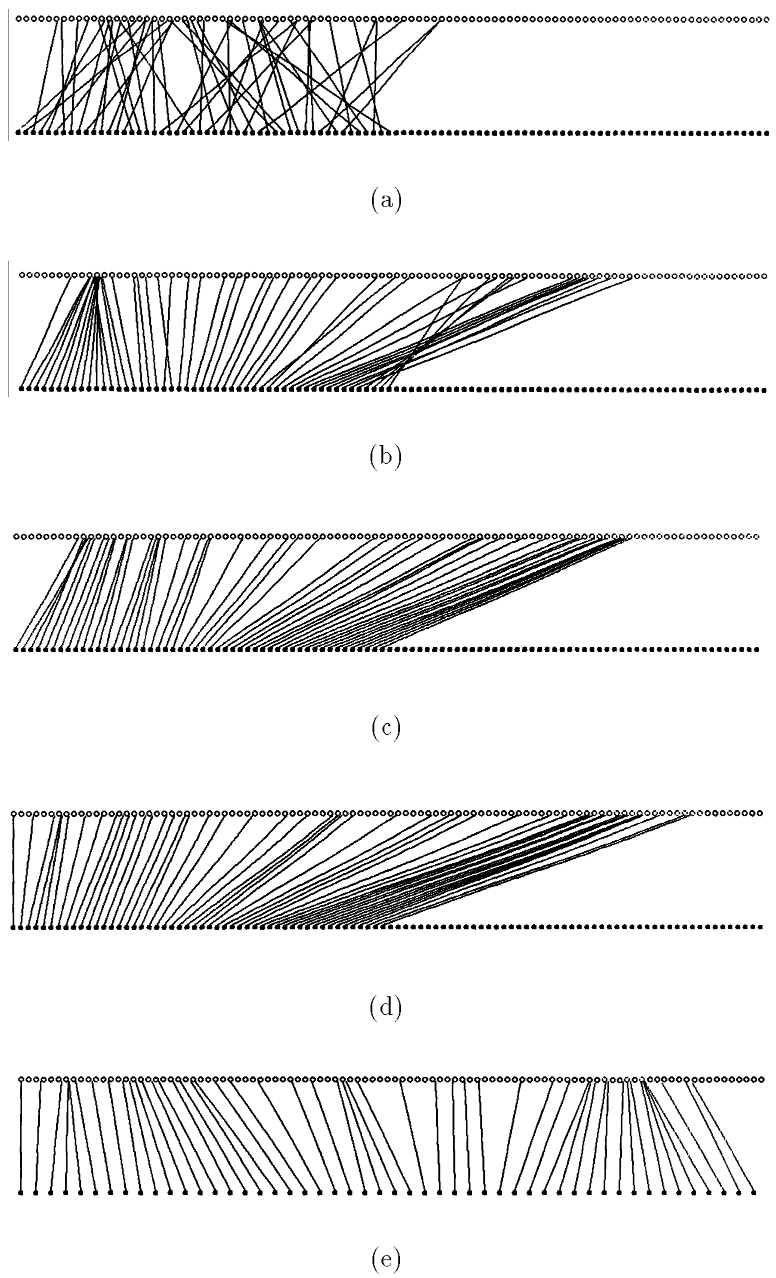

Figure 3-8: Map expansion following a lesion which removes the right half of the source map. Results are shown after (a) 0, (b) 100, (c) 1000, and (d) 10000 trials. (e) Same as (d), but with the remaining source neurons spaced apart to full breadth of the map.

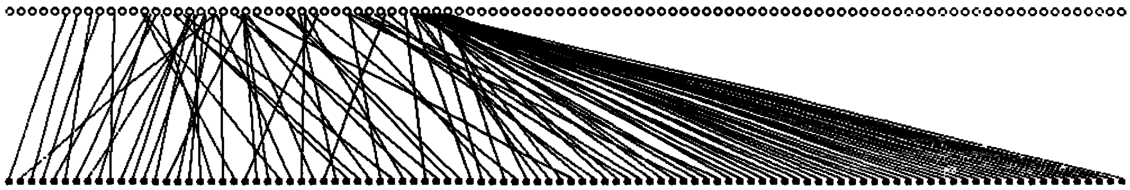

(a)

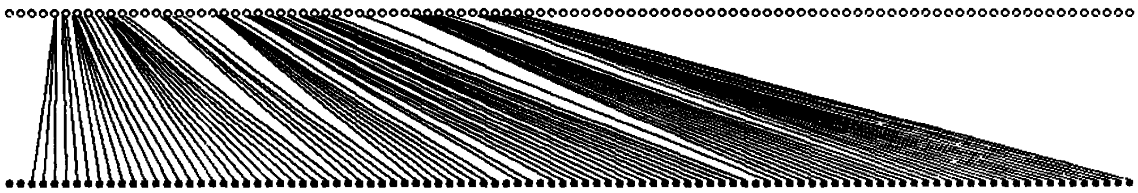

(b)

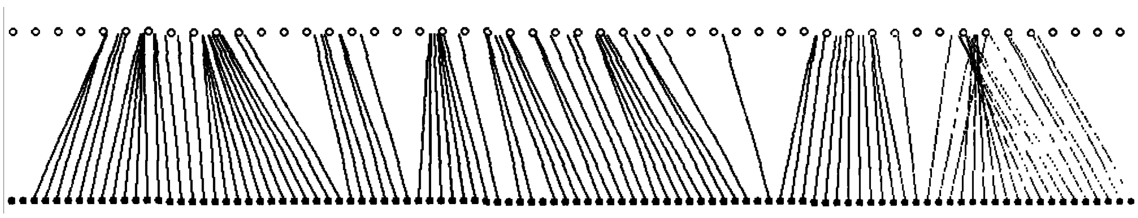

(c)

Figure 3-9: Map compression following a lesion which removes the right half of the target map. Axons which would normally connect to the missing portion of the target are initially bunched up along the edge of the lesion. Results are shown after (a) 0 and (b) 10000 trials. (c) Same as (b), but with the remaining target neurons spaced apart to full breadth of the map.

3.7 Discussion and Summary

Map formation in this simulation is accurate and robust, and provides a good match to experimental data, despite the use of an extremely simple neuron model. It may be that developmental phenomena such as map formation are relatively insensitive to detailed properties of the cell, either because their success is so important to the organism, or because these properties are in such flux during development. It is likely that modelling of more complex neural behaviors will require the inclusion of higher-order effects that appear not to be critical for topographic map formation.

Chemoaffinity, in this model, is assumed to create a rough initial map that is refined by an activity-based mechanism. An LTP-like learning process uses this rough map, together with correlations in source activity, to focus the axonal arbors into localized regions matching the detailed topography of the source map. The accuracy of the initial map is surprisingly unimportant in achieving an accurate final map, as long as the axonal projections of neighboring source neurons overlap. Competitive mechanisms produce activity-dependent map expansion.

The pattern of activity in the target cell layer is critical in determining the result of the map formation process. The biological process described in this paper results in an activity pattern that is ideal for producing rapid convergence to a detailed map.

Chapter 4

Mathematical Analysis of Map Formation

Chapter 3 presents a simulation of topographic map formation, along with experimental results of running that simulation in a variety of test conditions. In this chapter, the underlying mathematics are described in detail and analyzed.

The first section presents detailed equations describing the simulation, and gives constraints on the parameter values that ensure it will behave according to plan.

The second section derives a new learning rule which uses an activity-dependent decay as a competitive mechanism, and whose behavior is similar to that of input normalization given certain simplifying assumptions. Simulation results are presented which demonstrate that the new rule works well for map formation.

The third section addresses the question of the nature and stability of equilibrium states for the map formation process. An equation is derived showing the relationship between the final weights and the final target activity patterns. For the simple case with full connectivity between source and target and no lateral connections in the target, it is shown that the system is stable about an equilibrium point where all weights have the same value: $\forall_{i,j}\, w_{ij} = K/m$.

4.1 Description of Simulation

The network has a one-dimensional input layer with m nodes, which projects to a one-dimensional output layer with n nodes. At trial T, an input activity pattern $[a_0(T)..a_{m-1}(T)]$ is presented, and a target response (target activity pattern) $[o_0(T)..o_{n-1}(T)]$ is computed by simulating the spreading of activation via lateral connections in the target. The strength of the synaptic connection $w_{ij}(T)$ from input node j to target node i is then updated by a Hebbian learning rule (in the numerator) combined with a competitive mechanism (in the denominator).

$$w_{ij}(T+1) = \frac{w_{ij}(T) + \alpha\, A_{ij}(T)\, o_i(T)\, a_j(T)}{\frac{1}{K}\sum_{j=0}^{m-1}(w_{ij}(T) + \alpha\, A_{ij}(T)\, o_i(T)\, a_j(T))} \tag{4.1}$$

In this equation, α is the learning rate, $A_{ij}(T) = 1$ if there is a synapse from j to i and 0 otherwise, and K is the maximum synaptic input to a target node. The synaptic strengths w_{ij} are strictly excitatory; that is, $\forall_{i,j}\, w_{ij} \geq 0$.

Initial conditions for the synaptic connectivity $A_{ij}(0)$ and weights $w_{ij}(0)$ are determined using two control parameters, r and ϵ. r is the radius of the axonal arbor, and ϵ is the maximum position error. For each input node j, the topographically corresponding target location is $i = round[jn/m]$. An error ϵ_j for that projection is chosen randomly in a uniform distribution over the range $[-\epsilon..\epsilon]$. The initial connectivity is:[1]

$$A_{ij}(0) = \begin{cases} 1 & \text{if } j + \epsilon_j - r \leq j \leq j + \epsilon_j + r \\ 0 & \text{otherwise} \end{cases} \tag{4.2}$$

Synapses are removed if their strength goes below a minimum value, to prevent floating-point underflow errors in the simulation.

[1] Differences are calculated mod n for wraparound.

$$A_{ij}(T+1) = \begin{cases} 1 & \text{if } A_{ij}(T) = 1 \ \wedge \ w_{ij}(T) > \epsilon \\ 0 & \text{otherwise} \end{cases} \tag{4.3}$$

In lesion tests, where synapse formation is included, it takes a very simple form. The initial weight of a new synapse, $w_{ij}(T+1)$, is set to a random value. A new synapse is formed between a source node j and a target node to which it is not already connected when the synapse from j to a neighboring target node is strengthened:

$$A_{ij}(T+1) = \begin{cases} 1 & \text{if } (A_{ij}(T) = 1 \ \wedge \ w_{ij}(T) > \epsilon) \\ & \qquad \vee \ \Delta w_{(i-1)j}(T) > 0 \\ & \qquad\qquad \vee \ \Delta w_{(i+1)j}(T) > 0 \\ 0 & \text{otherwise} \end{cases} \tag{4.4}$$

Initial weights $w_{ij}(0)$ are set to random values where $A_{ij}(0) = 1$, and 0.0 otherwise. The weights are then normalized using the competitive mechanism from the learning rule. This mechanism ensures that the summed synaptic strength of all connections from the source layer to a given target node is constant, that is,

$$\sum_{k=0}^{m-1} w_{ik}(T) = K \tag{4.5}$$

When $K = 1.0$, the competitive mechanism is known as "input normalization."

The input activity $a_j(T)$ for a given trial consists of a contiguous activity cluster, containing $c(T)$ active nodes. The location of this cluster is chosen randomly. For most test runs, $c(T)$ is a constant, and the cluster location is chosen using a uniform distribution across the source map.

$$a_j(T) = \begin{cases} 1.0 & \text{if node } j \text{ is active} \\ 0.0 & \text{otherwise} \end{cases} \tag{4.6}$$

The target activity $o_i(T)$ for a given trial is determined by the time course of target activation within that trial. This time course is simulated by stepping the system through the trial with an intra-trial time step t, which is much shorter than the inter-trial step T. To get the total target activity for a trial, the activation at time t is summed over a time window of length τ, beginning at the stimulus presentation for that trial.

$$o_i(T) = \sum_{t=t_0}^{t_0+\tau} \phi_i(t) \tag{4.7}$$

$$\phi_i(t) = \begin{cases} \sum_{j=0}^{m-1} w_{ij}(T)\, A_{ij}(T)\, a_j(T) & t = t_0 \\ \sum_{j=0}^{n-1} \lambda_{ij} f_j(t-1) & t_0 < t \leq t_0 + \tau \end{cases} \tag{4.8}$$

$$f_j(t) = \begin{cases} 1.0 & \text{if } \phi_j(t) > \theta \\ 0.0 & \text{otherwise} \end{cases} \tag{4.9}$$

In these equations, $\phi_i(t)$ is the target activation at time step t within trial T, λ_{ij} is the lateral connection strength between target nodes j and i, and θ is the firing threshold for the target nodes.

The lateral connections λ_{ij} in the target are defined to be a symmetrical triangular ramp of radius ρ.[2]

$$\lambda_{ij} = \begin{cases} \Lambda \cdot \left(1 - \frac{|\,i-j\,| - 1}{\rho}\right) & \text{if } 0 < |\,i-j\,| \leq \rho \\ 0.0 & \text{otherwise} \end{cases} \tag{4.10}$$

The constant Λ is the summed connection strength of all lateral inputs to a single target node.

$$\Lambda = \Lambda_i = \sum_{j=0}^{n-1} \lambda_{ij} \tag{4.11}$$

[2]Differences are calculated mod n for wraparound.

4.1.1 Parameter Constraints

There are a large number of parameters in the system, which might at first glance make it look like a connectionist's nightmare. However, an analysis of these parameters gives rise to a simple set of constraints on their values, within which the simulation will behave according to plan. The basic parameters are:

- m (number of source nodes)
- n (number of target nodes)
- α (learning rate)
- K (competition limit)
- τ (length of time window for Hebbian learning)
- θ (firing threshold)
- Λ (summed lateral connection strength)
- ρ (radius of lateral connections)

Map Configuration

The map configuration was set at $m = n = 100$, with the ends wrapped to reduce edge effects, using one-dimensional maps. Using a one-dimensional map makes it possible to study effects over a longer distance in the map without the computation time becoming prohibitive.

Learning Parameters

The competition limit K is the sum of incoming synaptic strengths to a given target node. This limit must be set high enough to allow the target to fire in response to the source activity, or learning will not occur.

In the tests which use a uniform input activity cluster size, the competition limit is set relative to the cluster size to ensure that initial synaptic strengths are sufficient to induce firing in the target. The average initial projection strength is $K/2r$. For an activity cluster of size c, the maximum target activation at time t_0 is therefore $cK/2r$, to initiate target firing we require the following condition:

$$\frac{cK}{2r} > \theta \tag{4.12}$$

In these tests, an intermediate K value is used that requires, in the initial state, input projections from roughly half the source nodes to initiate firing in a target node.

$$K = \frac{4r\theta}{c} \tag{4.13}$$

The target activity function is designed to die out naturally within a small number of time steps, and the time window τ for Hebbian learning is to be longer than the maximum duration of the target activity.

The Hebb learning rate, α, must be set low enough to ensure convergence, but otherwise we want it as large as possible so that it will converge quickly.

The derivation in Section 4.2 assumes that incremental changes are very small. One concrete constraint on the learning rate, required if we are to accurately approximate the competition term with an activity-dependent decay, is

$$\frac{\alpha\, c_{max}\, o_{i\,max}}{K} \ll 1.0 \tag{4.14}$$

or

$$\alpha \ll \frac{4r\theta}{c^2 o_{i\,max}} \tag{4.15}$$

For example, if $c = 10$ and $r = 30$, assuming a maximum target activity of 50,

$$\alpha \ll \frac{4 \cdot 30 \cdot 1.0}{100 \cdot 50} = 0.024 \tag{4.16}$$

Parameters Affecting Target Activity

The firing threshold is normalized to 1.0, and other activity-related parameters are set in proportion to it.

The desired target activity will die out naturally over time, but persist longer toward the center of the projection than at its edges. Therefore, if all nodes within the lateral activation range are firing, a node should continue to fire, while nodes along the borders of an active region should cease firing. In the center of an active region, the activation is $\phi_i = \Lambda$.

The activation of a node at the edge of an active region (all nodes on one side firing, all nodes on the other quiet), on the other hand, should fall below threshold. This activation is $\phi_i = \Lambda/2$.

If we want target activity to die out from the edges, persisting longest in the center, the bounds for the lateral connection strengths are therefore

$$\theta < \Lambda < 2\theta \tag{4.17}$$

An intermediate value for Λ, 1.5, was used.

of the summed target activity pattern given different

The radius of the lateral activation curve, ρ, is less critical. The primary effect of this parameter is to smooth over variations in the input activity — a longer radius increases the ability to recover if individual nodes within an active region do not initially reach firing threshold. It also smooths out the summed activity pattern, making it more similar to a gaussian, while shorter values of ρ make the activity curve more triangular.

The value used in the simulation was $\rho = 5$.

Test Conditions

A number of parameters were varied to create different situations for testing. These include

- r (radius of initial axonal arbors)
- ϵ (maximum initial position error)
- $c(T)$ (size of input activity clusters)
- distribution of locations of input activity clusters

The first set of tests was designed to test the robustness of the learning algorithm. The accuracy of the chemical markers and the source activity pattern was varied to create different learning conditions.

The initial radius of the distribution was set at a breadth that would ensure overlap with the goal location, to avoid the need to model new synapse formation. The corresponding constraint is $r > \epsilon$.

In a map that wraps around on itself, we also need to ensure that the initial position error is not large enough for the axonal arbors to wrap around on themselves, as the wraparound is intended to simulate a very large map, not a circular one. To prevent this problem, we need the following constraint:

$$2(r + \epsilon) < n \tag{4.18}$$

To test ϵ values between 0 and 20, the projection radius r was set at 30. It would be necessary to increase the map size in order to test larger position errors.

The size and distribution of input activity clusters was tested at constant levels between $c = 2$ and $c = 10$. The simulation was also tested using input activity cluster sizes that varied randomly within that range. The distribution of input activity cluster locations was uniform in the initial tests, which should result in a map with uniform spacing. Tests of map expansion and contraction used non-uniform distributions.

4.2 Derivation of Activity-Dependent Decay

This section shows how input normalization can be approximated by an activity-dependent decay term. Although no biological process observed to date is known to produce an activity-dependent decay, it nonetheless allows for a simple biological implementation, due to the local availability at the synapse of information about the target activity.

Oja [53] showed that vector input normalization can be approximated (in the limit where α is small) by an activity-dependent decay, given the assumption that there are no lateral connections in the target map.

The analysis presented here shows that the decay term for input normalization cannot be made completely independent of input activity in the presence of lateral connections. However, if we allow the normalization constant K to vary slowly over time and across the surface of the target map, we can derive a new learning rule which is similar to our old rule but which uses an activity-dependent decay. This new rule is simulated to demonstrate that it does produce reasonable competitive behavior, and that the summed input strengths, although variable, nonetheless remain close to K.

Our original learning rule is

$$w_{ij}(T+1) = \frac{w_{ij}(T) + \alpha\, A_{ij}(T)\, o_i(T)\, a_j(T)}{\frac{1}{K}\sum_{j=0}^{m-1}(w_{ij}(T) + \alpha\, A_{ij}(T)\, o_i(T)\, a_j(T))} \tag{4.19}$$

Because of the input normalization,

$$\sum_{j=0}^{m-1} w_{ij}(T) = K \tag{4.20}$$

which means we can convert our learning rule to

$$w_{ij}(T+1) = \frac{w_{ij}(T) + \alpha\, A_{ij}(T)\, o_i(T)\, a_j(T)}{1 + \dfrac{\alpha\, o_i(T)}{K} \displaystyle\sum_{j=0}^{m-1} A_{ij}(T)\, a_j(T)} \tag{4.21}$$

All terms in

$$\frac{\alpha o_i(T)}{K} \sum_{j=0}^{m-1} A_{ij}(T)\, a_j(T) \tag{4.22}$$

are finite, so this term can be made arbitrarily small by a suitable choice of α. In this case, we can make the following series expansion:

$$\frac{1}{1 + \dfrac{\alpha o_i(T)}{K} \displaystyle\sum_{j=0}^{m-1} A_{ij}(T)\, a_j(T)} = 1 - \frac{\alpha\, o_i(T)}{K} \sum_{j=0}^{m-1} A_{ij}(T)\, a_j(T) + O[\alpha^2] \tag{4.23}$$

This transforms our learning rule to

$$\begin{aligned} & w_{ij}(T+1) \\ &= (w_{ij}(T) + \alpha A_{ij}(T)\, o_i(T)\, a_j(T)) \left(1 - \frac{\alpha\, o_i(T)}{K} \sum_{j=0}^{m-1} A_{ij}(T)\, a_j(T) + O[\alpha^2]\right) \\ &= w_{ij}(T) + \alpha A_{ij}(T)\, o_i(T)\, a_j(T) - w_{ij}(T) \frac{\alpha\, o_i(T)}{K} \sum_{j=0}^{m-1} A_{ij}(T)\, a_j(T) + O[\alpha^2] \\ &\approx w_{ij}(T) + \alpha A_{ij}(T)\, o_i(T)\, a_j(T) - w_{ij}(T)\, o_i(T) \frac{\alpha\, N_i(T)}{K} \end{aligned} \tag{4.24}$$

where

$$N_i(T) = \sum_{j=0}^{m-1} A_{ij}(T)\, a_j(T) \tag{4.25}$$

The real appeal of an activity-dependent decay term is that it is dependent *only* on target activity, and therefore has a superior claim to biological plausibility. If we assume a constant input cluster size and full connectivity between source and target maps, then $N_i(T)$ is constant, and in this case the decay term becomes a pure activity-dependent decay.

In more realistic situations, however, $N_i(T)$ will vary due to variations in the size of the input activity cluster and the connectivity between the two maps.

Up to this point, our derivation is quite similar to the one presented in [53], but this is as far as Oja takes us. In Oja's derivation, the decay term was made independent from the input activities by assuming that the output is simply the weighted sum of the inputs; that is,

$$o_i(T) = \sum_{j=0}^{m-1} w_{ij}(T) a_j(T) \tag{4.26}$$

which is only the case if there are no lateral connections. Because of the presence of lateral connections in this simulation, we cannot make this simplification.

If we average the effect of the decay term over many time steps, our learning rule can be further approximated as:

$$w_{ij}(T+1) \approx w_{ij}(T) + \alpha A_{ij}(T)\, o_i(T)\, a_j(T) - w_{ij}(T)\frac{\alpha}{K}\left\langle o_i(T)\, N_i(T)\right\rangle \tag{4.27}$$

where

$$\left\langle o_i(T)\, N_i(T)\right\rangle = \left\langle o_i(T)\right\rangle \left\langle N_i(T)\right\rangle + \mathrm{Cov}\left[o_i(T), N_i(T)\right] \tag{4.28}$$

The angle brackets $\langle\rangle$ denote expected value, and $\mathrm{Cov}[x, y]$ is the covariance of x and y. Substituting back in to our learning rule, and replacing $\langle o_i(T)\rangle$ with $o_i(T)$, we obtain

$$w_{ij}(T+1) \approx w_{ij}(T) + \alpha A_{ij}(T)\, o_i(T)\, a_j(T) - w_{ij}(T)\, o_i(T) \frac{\alpha\, N_i'(T)}{K} \tag{4.29}$$

where

$$N_i'(T) = \langle N_i(T) \rangle + \frac{\mathrm{Cov}[o_i(T), N_i(T)]}{\langle o_i(T) \rangle} \tag{4.30}$$

with the averages taken over a large time window around T.

If we average $N_i'(T)$ over both i and T and replace it by a constant $N' = \langle N_i'(T) \rangle$, we obtain a new learning rule with a pure activity-dependent decay.

$$w_{ij}(T+1) = w_{ij}(T) + \alpha\, A_{ij}(T)\, o_i(T)\, a_j(T) - w_{ij}(T)\, o_i(T) \frac{\alpha N'}{K} \tag{4.31}$$

The behavior of the new learning rule is approximately equivalent to the old rule if the learning rate is small and if $N_i'(T)$ does not vary over time or across the surface of the map.

However, the summed strength of the inputs to a single target node is no longer explicitly normalized to K, so if the actual value of $N_i'(T)$ differs from our assumed value N', the summed input strength will converge to a new value,

$$K_i(T) = K \frac{N_i'(T)}{N'} \tag{4.32}$$

This gives us a learning rule in which the summed input strength to a target node i is maintained at a value which may vary across the surface of the map, or which may change slowly over time.

Two questions are of interest for evaluating this new learning rule. One obvious question is how similar it is to input normalization, which is known to work well as a competitive mechanism. But other competitive processes which do not normalize the

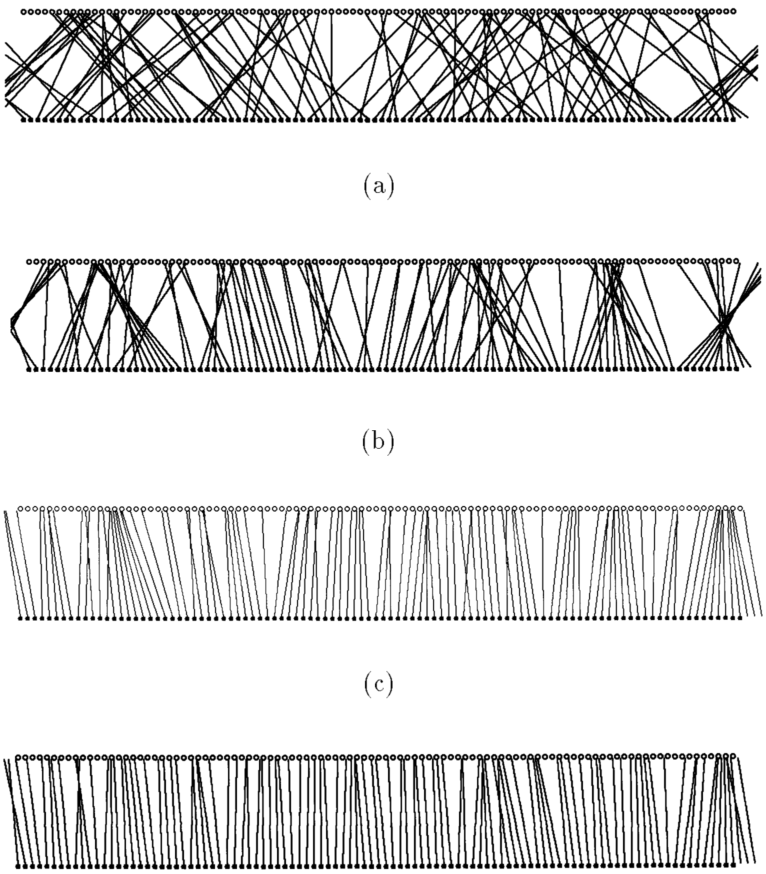

(a)

(b)

(c)

(d)

Figure 4-1: Map formation using activity-dependent decay as a competitive mechanism, with an initial error of ± 20 and an activity cluster size of 5. Results are shown after (a) 0, (b) 100, (c) 1000, and (d) 10000 trials.

(a)

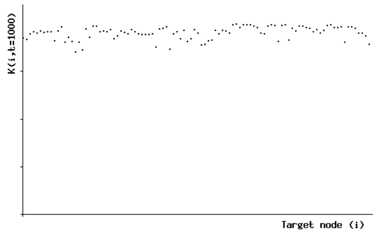

(c)

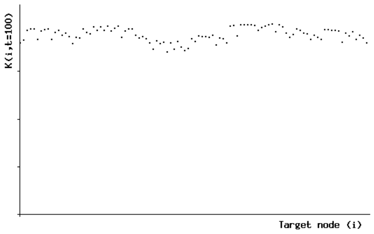

(b)

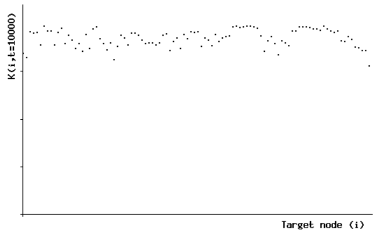

(d)

Figure 4-2: Variations in $K_i(T)$ across the target map after (a) 0, (b) 100, (c) 1000, and (d) 10000 trials.

inputs to a target node may work equally well. So we must ask, as a separate question, how well this activity-dependent decay term works as a competitive mechanism. Figure 4-1 shows the results of a map formation test using an activity-dependent decay in the place of input normalization. Figure 4-2 shows a graph of $K_i(t)$ across the target map at four different times during map formation. These results indicate that activity-dependent decay works well for map formation, and although the values of K_i do spread out somewhat, they appear to remain within a relatively narrow range around a stable mean value.

4.3 Equilibrium Solutions and Stability

This section derives equations describing the dynamic behavior of the weight vectors over the course of a learning simulation. General solutions are given for the equilibrium solutions, and an equation is given which can be used to determine the stability of a known equilibrium solution.

In the case of uniform input activity and full connectivity, it is shown that the weights w_{ij} have an equilibrium solution where their values are proportional to the sum of the target i's response to all input activity patterns in which the node j is active, weighted by the probability of that input activity pattern. This means that the process which generates the target activity pattern also determines the shape (breadth and distribution of synaptic weights) of the final axonal arbors.

It is also shown that, for the case where there is uniform input activity, full connectivity, and no lateral connections, the map formation process will converge to a solution where all weights are equal.

4.3.1 Equilibrium Solution

If we assume that incremental changes are very small, and sum a large number of time steps t into a single epoch E, we can approximate the system as follows:

$$
\begin{aligned}
w_{ij}(E+1) &\approx \frac{w_{ij}(E) + \alpha \sum_{p \in P} \mathbf{P}[p]\, A_{ij}(E)\, o_i(p,E)\, a_j(p)}{\frac{1}{K} \sum_{p \in P} \mathbf{P}[p] \left(w_{ij}(E) + \alpha o_i(p,E) \sum_{k=0}^{m-1} A_{ik}(E)\, a_k(p) \right)} \\
&= \frac{w_{ij}(E) + \alpha \sum_{p \in P} \mathbf{P}[p]\, A_{ij}(E)\, o_i(p,E)\, a_j(p)}{1 + \frac{\alpha}{K} \cdot \sum_{p \in P} \mathbf{P}[p]\, o_i(p,E) \sum_{k=0}^{m-1} A_{ik}(E)\, a_k(p)} \qquad (4.33)
\end{aligned}
$$

where P is the set of all possible input patterns, $a_j(p)$ and $o_i(p)$ are the source and target activities for pattern p, and $\mathbf{P}[]$ denotes "probability of".

We can define functions to represent the Hebbian and Competition terms in this equation as follows:

$$
\begin{aligned}
H_{ij}(E) &= \alpha \sum_{p \in P} \mathbf{P}[p]\, A_{ij}(E)\, o_i(p,E)\, a_j(p) \qquad (4.34) \\
C_i(E) &= \frac{\alpha}{K} \sum_{p \in P} \mathbf{P}[p]\, o_i(p,E) \sum_{k=0}^{m-1} A_{ik}(E)\, a_k(p) \qquad (4.35) \\
w_{ij}(E+1) &\approx \frac{w_{ij}(E) + H_{ij}(E)}{1 + C_i(E)} \qquad (4.36)
\end{aligned}
$$

Now we can determine the equilibrium states, in terms of $H_{ij}(E)$ and $C_i(E)$, by setting $w_{ij,eq} = w_{ij}(E+1) = w_{ij}(E)$. This gives us the following:

$$
\begin{aligned}
w_{ij,eq} &= \frac{H_{ij,eq}}{C_{i,eq}} \qquad (4.37) \\
H_{ij,eq} &= \alpha \sum_{p \in P} \mathbf{P}[p]\, A_{ij,eq}\, o_{i,eq}(p)\, a_j(p) \qquad (4.38)
\end{aligned}
$$

$$C_{i,eq} = \frac{\alpha}{K} \sum_{p \in P} \mathbf{P}[p] \, o_{i,eq}(p) \sum_{k=0}^{m-1} A_{ik,eq} \, a_k(p) \tag{4.39}$$

4.3.2 Stability of Equilibrium Solutions

To determine stability, we must look at the value of $\Delta w_{ij}(E) = w_{ij}(E+1) - w_{ij}(E)$ in the neighborhood of the equilibrium solutions. Liapunov's method can then be used to determine the stability of a known equilibrium solution. To apply this method, we linearize the equation for $\Delta w_{ij}(E)$ around around a known equilibrium solution, then solve for the characteristic roots of the variance matrix. If all real components of those roots are negative, then it is possible to construct a Liapunov function for the solution, and the state is stable.

Our variational equation is

$$\begin{aligned} \Delta w_{ij}(E) &= w_{ij}(E+1) - w_{ij}(E) \\ &= \frac{w_{ij}(E) + H_{ij}(E)}{1 + C_i(E)} - w_{ij}(E) \\ &= \frac{H_{ij}(E)}{1 + C_i(E)} - \frac{C_i(E)}{1 + C_i(E)} w_{ij}(E) \end{aligned} \tag{4.40}$$

The stability of this system cannot be determined in the general case, as the target activity, on which both $H_{ij}(E)$ and $C_i(E)$ depend, cannot be found in general except by simulation. However, we can determine stability for certain special cases. An example is given in Section 4.3.4.

4.3.3 Equilibrium Solution with Uniform Input Activity

In this section we solve for the equilibrium solutions in a simplified case, where the the input activity cluster size is a constant c, and the input activity is uniformly distributed across the source map. In this case, for a map with its ends wrapped, there are m possible input patterns which contain c contiguous active nodes. Each of these patterns occurs with probability $\mathbf{P}[p] = 1/m$. These are the conditions under which the first set of tests was run.

Under these conditions, the equations simplify to

$$
\begin{aligned}
H_{ij}(E) &= \frac{\alpha}{m} \sum_{p \in P} A_{ij}(E)\, o_i(p, E)\, a_j(p) \\
&= \frac{\alpha}{m} \sum_{p \in P_j} A_{ij}(E)\, o_i(p, E) && (4.41) \\
C_i(E) &= \frac{\alpha}{K\, m} \sum_{p \in P} o_i(p, E) \sum_{k=0}^{m-1} A_{ik}(E)\, a_k(p) && (4.42) \\
w_{ij}(E+1) &= \frac{w_{ij}(E) + \frac{\alpha}{m} \sum_{p \in P_j} A_{ij}(E)\, o_i(p, E)}{1 + \frac{\alpha}{K\, m} \sum_{p \in P} o_i(p, E) \sum_{k=0}^{m-1} A_{ik}(E)\, a_k(p)} && (4.43)
\end{aligned}
$$

and

$$
\begin{aligned}
H_{ij,eq} &= \frac{\alpha}{m} \sum_{p \in P_j} A_{ij,eq}\, o_{i,eq}(p) && (4.44) \\
C_{i,eq} &= \frac{\alpha}{K\, m} \sum_{p \in P} o_{i,eq}(p) \sum_{k=0}^{m-1} A_{ik,eq}\, a_k(p) && (4.45) \\
w_{ij,eq} &= \frac{H_{ij,eq}}{C_{i,eq}} \\
&= \frac{K \cdot \sum_{p \in P_j} A_{ij,eq}\, o_{i,eq}(p)}{\sum_{p \in P} o_{i,eq}(p) \sum_{k=0}^{m-1} A_{ik,eq}\, a_k(p)} && (4.46)
\end{aligned}
$$

where P_j is the set of all input patterns in which node j is active.

In addition, we will assume that we have full connectivity between the two layers,[3] so that $A_{ij} = 1$, giving us:

$$H_{ij}(E) = \frac{\alpha}{m} \sum_{p \in P_j} o_i(p, E) \tag{4.47}$$

$$\begin{aligned} C_i(E) &= \frac{\alpha}{K\, m} \sum_{p \in P} o_i(p, E) \sum_{k=0}^{m-1} a_k(p) \\ &= \frac{\alpha\, c}{K\, m} \sum_{p \in P} o_i(p, E) \end{aligned} \tag{4.48}$$

$$w_{ij}(E+1) = \frac{w_{ij}(E) + \frac{\alpha}{m} \sum_{p \in P_j} o_i(p, E)}{1 + \frac{\alpha\, c}{K\, m} \sum_{p \in P} o_i(p, E)} \tag{4.49}$$

and

$$H_{ij,eq} = \frac{\alpha}{m} \sum_{p \in P_j} o_{i,eq}(p) \tag{4.50}$$

$$C_{i,eq} = \frac{\alpha\, c}{K\, m} \sum_{p \in P} o_{i,eq}(p) \tag{4.51}$$

$$w_{ij,eq} = \frac{K \sum_{p \in P_j} o_{i,eq}(p)}{c \sum_{p \in P} o_{i,eq}(p)} \tag{4.52}$$

The weight between any source node j and target node i at equilibrium will be proportional to the ratio between the expected activity at i when j is active and the average activity at i.

If we assume a uniform solution, where all arbors have the same shape, then the

[3] A node with a limited synaptic arbor will behave as if it had full connectivity as long as its arbor overlaps the same region in the target as other simultaneously active source nodes.

average activity at i is the same for all i, and our weight equation at equilibrium simplifies still further, to

$$w_{ij,eq} \propto \sum_{p \in P_j} o_{i,eq}(p) \tag{4.53}$$

Since $o_{i,eq}(p)$ is itself dependent on the $w_{ij,eq}$'s, this equation can be expanded to give a solution purely in terms of the weights and the target activity function.

$$\begin{aligned}
\vec{o}_{eq}(p) &= \vec{F}[W_{eq}\vec{a}(p)] \qquad (4.54)\\
W_{eq} &\propto \begin{bmatrix} \sum_{p \in P_0} \vec{o}_{eq}(p)^T \\ \vdots \\ \sum_{p \in P_{m-1}} \vec{o}_{eq}(p)^T \end{bmatrix} \\
&= \begin{bmatrix} \sum_{p \in P_0} \vec{F}[W_{eq}\vec{a}(p)]^T \\ \vdots \\ \sum_{p \in P_{m-1}} \vec{F}[W_{eq}\vec{a}(p)]^T \end{bmatrix} \qquad (4.55)
\end{aligned}$$

where $\vec{o}_{eq}(p)$ is the equilibrium target activity (in vector form) for pattern p, $\vec{F}[\vec{x}]$ is a function which returns the summed target activity given an initial activation of $\vec{x}$, and W_{eq} is the weight matrix.

Given a particular target activation function $\vec{F}$, we can calculate W_{eq} for the uniform solution, and determine its dependency on the ratio of the competition limit K and the cluster size c.

4.3.4 Equilibrium Solution with No Lateral Connections

In this section, we will consider the case where we have no lateral connections. Now each target node operates independently, so we only need to consider one target node, with inputs $\vec{a}(p) = [a_0(p) \;\; a_1(p) \;\cdots\; a_{m-1}(p)]$, weights $\vec{w}(E) = [w_0(E) \;\; w_1(E) \;\cdots\; w_{m-1}(E)]$, and output activity

$$o(p,E) = \sum_{0}^{m-1} w_j(E)\, a_j(E) = \vec{w}(E)^T\, \vec{a}(p) \tag{4.56}$$

Our learning rule, in this case, simplifies to

$$\begin{aligned}
\vec{H}(E) &= \alpha \sum_{p \in P} \mathbf{P}[p]\, \vec{w}(E)^T\, \vec{a}(p)\, \mathrm{A}(E)\, \vec{a}(p) \\
&= \alpha\, \mathrm{A}(E) \left(\sum_{p \in P} \mathbf{P}[p]\, \vec{a}(p)\, \vec{a}(p)^T \right) \vec{w}(E) \\
&= \alpha\, \mathrm{A}(E)\, \mathrm{M}\, \vec{w}(E) \qquad (4.57) \\
C(E) &= \frac{\alpha}{K} \sum_{p \in P} \mathbf{P}[p]\, \vec{w}(E)^T\, \vec{a}(p)\, \vec{A}(E)^T\, \vec{a}(p) \\
&= \frac{\alpha}{K}\, \vec{A}(E)^T \left(\sum_{p \in P} \mathbf{P}[p]\, \vec{a}(p)\, \vec{a}(p)^T \right) \vec{w}(E) \\
&= \frac{\alpha}{K}\, \vec{A}(E)^T\, \mathrm{M}\, \vec{w}(E) \qquad (4.58) \\
\vec{w}(E+1) &\approx \frac{\vec{w}(E) + \vec{H}(E)}{1 + C(E)} \\
&= \frac{\vec{w}(E) + \alpha\, \mathrm{A}(E)\, \mathrm{M}\, \vec{w}(E)}{1 + \frac{\alpha}{K}\, \vec{A}(E)^T\, \mathrm{M}\, \vec{w}(E)} \qquad (4.59)
\end{aligned}$$

where $\mathrm{A}(E)$ is an m by m matrix, with entries

$$\mathrm{A}_{ij}(E) = \begin{cases} A_j(E) & \text{if } i = j \\ 0 & \text{otherwise} \end{cases} \tag{4.60}$$

and

$$\mathrm{M} = \sum_{p \in P} \mathbf{P}[p]\, \vec{a}(p)\, \vec{a}(p)^T \tag{4.61}$$

Solving for the equilibrium states, we get

$$\vec{H}_{eq} = \alpha\, \mathrm{A}_{eq}\, \mathrm{M}\, \vec{w}_{eq} \tag{4.62}$$

$$C_{eq} = \frac{\alpha}{K}\, \vec{A}_{eq}^T\, \mathrm{M}\, \vec{w}_{eq} \tag{4.63}$$

$$\vec{w}_{eq} = \frac{K\, \mathrm{A}_{eq}\, \mathrm{M}\, \vec{w}_{eq}}{\vec{A}_{eq}^T\, \mathrm{M}\, \vec{w}_{eq}} \tag{4.64}$$

This system is linear, and we can write its equilibrium solution as

$$\mathrm{A}_{eq}\, \mathrm{M}\, \vec{w}_{eq} = \frac{\vec{A}_{eq}^T\, \mathrm{M}\, \vec{w}_{eq}}{K}\, \vec{w}_{eq} \tag{4.65}$$

where

$$\frac{\vec{A}_{eq}^T\, \mathrm{M}\, \vec{w}_{eq}}{K} = \frac{C_{eq}}{\alpha} \tag{4.66}$$

is an eigenvalue of the matrix $\mathrm{A}_{eq}\mathrm{M}$, and $\vec{w}_{eq}$ is the corresponding eigenvector.

Stability with Uniform Input Activity

If we assume a constant input activity cluster size c, full connectivity, and a uniform input activity distribution, we can solve for $C(E)$. In this case,

$$\mathrm{M} = \frac{1}{m} \sum_{p \in P} \vec{a}(p)\, \vec{a}(p)^T \tag{4.67}$$

$$\vec{A}(E) = \vec{n} \tag{4.68}$$

$$\mathrm{A}(E) = \mathrm{I} \tag{4.69}$$

where $\vec{n}$ is a vector of all ones, and

$$\begin{aligned} C(E) &= \frac{\alpha}{K} \vec{A}(E)^T \, \mathrm{M} \, \vec{w}(E) \\ &= \frac{\alpha}{Km} \sum_{p \in P} \vec{n}^T \, \vec{a}(p) \, \vec{a}(p)^T \, \vec{w}(E) \end{aligned} \tag{4.70}$$

We can make the following substitutions in this equation:

$$\vec{n}^T \, \vec{a}(p) = c \tag{4.71}$$

$$\sum_{p \in P} \vec{a}(p)^T = c\vec{n}^T \tag{4.72}$$

$$\vec{n}^T \, \vec{w}(E) = K \tag{4.73}$$

at which point $C(E)$ can be seen to be a constant:

$$C(E) = \frac{\alpha \, c^2}{m} \tag{4.74}$$

$\vec{H}(E)$, similarly, can be simplified as follows:

$$\begin{aligned} \vec{H}(E) &= \frac{\alpha}{m} \left(\sum_{p \in P} \vec{a}(p) \, \vec{a}(p)^T \right) \vec{w}(E) \\ &= \frac{\alpha}{m} \mathrm{M}' \, \vec{w}(E) \end{aligned} \tag{4.75}$$

where

$$\mathrm{M}' = \sum_{p \in P} \vec{a}(p) \, \vec{a}(p)^T \tag{4.76}$$

The eigenvalue in this case is just

$$\frac{C_{eq}}{\alpha} = \frac{c^2}{m} \tag{4.77}$$

To determine stability, we want to look at the variation in $\Delta\vec{w}$ in the neighborhood of the equilibrium states. In this case the system is linear, so we can solve for $\Delta\vec{w}$ in general, as follows:

$$\begin{aligned}
\Delta\vec{w}(E) &= \frac{\vec{H}(E)}{1+C(E)} - \frac{C(E)}{1+C(E)}\vec{w}(E) \\
&= \frac{\frac{\alpha}{m}\,\mathrm{M}'\,\vec{w}(E)}{1+\frac{\alpha\, c^2}{m}} - \frac{\frac{\alpha\, c^2}{m}}{1+\frac{\alpha\, c^2}{m}}\vec{w}(E) \\
&= \frac{\frac{\alpha}{m}}{1+\frac{\alpha c^2}{m}}\,(\mathrm{M}' - c^2\mathrm{I})\,\vec{w}(E)
\end{aligned} \tag{4.78}$$

The stability of the equilibrium points can be determined by examining the eigenvalues of the matrix $\mathrm{M}' - c^2\mathrm{I}$. This matrix is symmetric, therefore all its eigenvalues are real. It is stable if all its eigenvalues are less than or equal to zero.

If we set $m = 5$ and $c = 2$, we find that the matrix M is

$$\mathrm{M} = \frac{1}{m}\begin{bmatrix} 2 & 1 & 0 & 0 & 1 \\ 1 & 2 & 1 & 0 & 0 \\ 0 & 1 & 2 & 1 & 0 \\ 0 & 0 & 1 & 2 & 1 \\ 1 & 0 & 0 & 1 & 2 \end{bmatrix}$$

The eigenvalue in this case is $c^2/m = 4/5$, and the corresponding eigenvector is $\vec{w} = (K/5)\vec{n}$. That is to say, all weights are the same at equilibrium. Now, we consider the variational matrix to determine stability.

$$\mathrm{M}' - c^2\mathrm{I} = \begin{bmatrix} -2 & 1 & 0 & 0 & 1 \\ 1 & -2 & 1 & 0 & 0 \\ 0 & 1 & -2 & 1 & 0 \\ 0 & 0 & 1 & -2 & 1 \\ 1 & 0 & 0 & 1 & -2 \end{bmatrix}$$

This matrix is negative semidefinite, so the system is stable, but not asymptotically stable.

Evolution of the Weight Vector

An interesting property of map formation in this system can be seen by looking at the evolution of the weight vector over time. Combining Equations 4.36, 4.47, and 4.74 and considering only a single target node, we find

$$w_j(E+1) = \frac{w_j(E) + \dfrac{\alpha}{m} \sum_{p \in P} \vec{w}(E)^T \, \vec{a}(p)}{1 + \dfrac{\alpha c^2}{m}} \tag{4.79}$$

If we set $c = 2$, this equation becomes

$$\begin{aligned} w_j(E+1) &= \frac{w_j(E) + \dfrac{\alpha}{m}(w_{j-1}(E) + 2w_j(E) + w_{j+1}(E))}{1 + \dfrac{4\,\alpha}{m}} \\ &= \frac{1 + \dfrac{2\,\alpha}{m}}{1 + \dfrac{4\,\alpha}{m}} w_j(E) + \frac{\dfrac{\alpha}{m}}{1 + \dfrac{4\,\alpha}{m}} (w_{j-1}(E) + w_{j+1}(E)) \end{aligned} \tag{4.80}$$

What this means is that each of the weights w_j is continuously being averaged with its neighbors. This results in a gradual spreading out of the arbor over time,